Sensors and Materials, Vol. 34, No. # (2022) 1–##
MYU Tokyo

S & M ####

Development and Application of Riding Profiler for Roughness Evaluation on Bicycle Riding Surfaces

Wuguang Lin,[1] Yu Dong,[1] Xue Ren,[1] Hao Han,[1] and YooSeok Jung[2*]

[1]College of Transport and Communications, Shanghai Maritime University,
1550 Haigang Ave., Shanghai 201306, P. R. China
[2]Korea Institute of Civil Engineering and Building Technology,
283 Goyang-daero, Ilsanseo-gu, Goyang-si, Gyeonggi-do 10223, Rep. of Korea

(Received June 16, 2021; accepted February 28, 2022; online published May 12, 2022)

Keywords: bicycle lane, roughness, riding profiler, vertical acceleration, acceleration interference, riding comfort

In recent years, the promotion of green travel and the emergence of bicycle sharing have dramatically increased the population of people traveling by bicycle in China. Bicycle sharing has become an indispensable daily means of travel for some people. Therefore, the ride comfort and safety of bicycle lanes should be paid more attention. Toward meeting the demand for smooth bicycle lanes, we propose a new method of testing the roughness of bicycle lanes based on the riding condition and explore the possibility of its realization. A riding profiler is assembled and designed, and its test repeatability is verified by repeated measurements. The riding profiler is also applied to different pavement types with various speeds for roughness testing. The results demonstrate that the speed and pavement type affect the vibration acceleration and vertical displacement during riding, and the greater the riding speed, the stronger the vibration sensation. In addition, the vibration is strongest when riding on concrete block pavement and weakest on dense asphalt pavement. On the basis of the test results, the acceleration interference is taken as an evaluation index to analyze riding comfort under different conditions.

1. Introduction

Over the past few decades, the number of automobiles worldwide has increased sharply owing to automobile-oriented urban planning and policies, resulting in problems such as air pollution, traffic jams, fossil fuel shortages, climate change, and road traffic accidents. In response, the demand for eco-friendly transportation has increased. Bicycles are representative of such transportation. As the supply of bicycles has exploded, new forms of business such as bicycle sharing and mobility as a service (MaaS) businesses have emerged, resulting in an increase in bicycle traffic. With the increasing number of bicycle users, interest in the comfort of bicycle riding is increasing with the smoothness of the surface, such as the highway pavement, affecting the riding comfort.

*Corresponding author: e-mail: yooseok@kict.re.kr

ISSN 0914-4935

American Society for Testing and Materials (ASTM) E867 defines roughness as "the vertical deviation of the road surface from the ideal plane". This deviation affects the dynamic characteristics of vehicles, driving quality, dynamic load on the road surface, and drainage.[1] Dozens of evaluation indicators have been adopted by different countries and industries owing to different levels of understanding the concept of roughness. Indexes of roughness can be classified into two categories: vehicle response indexes and direct surface roughness distribution indexes. Vehicle response indexes include international roughness index (IRI) and quarter index (QI), and direct surface roughness distribution indexes include slope variance (SV) and root mean square vertical acceleration (RMSVA).[2] IRI is the most commonly used index worldwide to describe the surface roughness of longitudinal sections and is used to evaluate and manage road systems. It is also used as a measure of road surface performance, which is related to the driving quality, dynamic wheel load, and running speed. According to Sayers and Karamihas,[3] IRI is highly correlated with vertical acceleration and tire load; vertical acceleration is associated with ride quality and tire load is related to vehicle controllability and safety.

However, it is difficult to use IRI to evaluate bicycle lanes on automobile roads. Generally, a passenger car runs at a speed of 40–180 km/h and can accommodate 4–6 passengers. It is equipped with a suspension system and internal seats, which reduce the impact of road undulation on passengers. In contrast, a bicycle runs at a speed of 10–40 km/h, can carry up to two persons, and is not equipped with a suspension system. Therefore, for the same road section, bicycle and car users will have different feedback perceptions due to the different characteristics of their vehicles.

Conventional tools and methods for testing pavement roughness include three-meter ruler roughness measuring instruments, vehicular bump integrators, continuous road roughness meters, and laser displacement sensors. A three-meter ruler roughness measuring instrument is simple and easy to operate but relatively laborious and time-consuming. This method is usually used for measuring and controlling the roughness during construction. A vehicular bump integrator has an inefficient calibration process.[4] The testing results of the continuous road roughness meter and three-meter ruler roughness measuring instrument are related to the lengths of their brackets and rulers, and can only reflect the wavelet components. For the continuous road roughness meter, the measuring results are greatly affected by the measuring speed. Therefore, both methods are inefficient.[5] Laser displacement sensors have high precision and speed. However, they also have many shortcomings, such as strict requirements for the test environment, the use of accelerometers to deal with the impact of the bumpiness of the vehicle itself, and desynchronization.[6] Thus, each of these test methods has its own advantages and disadvantages. In addition, the roughness cannot be directly measured from the geometric characteristics of the bicycle lane.

Therefore, an inexpensive, efficient, and accurate measurement method for bicycle lanes should be developed. Smartphone technology for testing road conditions has been accepted as a means of evaluating road quality by transportation authorities of many countries.[7–10] González *et al*.[11] proposed a method of using acceleration sensors fixed in specific vehicles to collect the data used to evaluate road conditions. Douangphachanh and Oneyama[12] used an acceleration sensor and the global positioning system (GPS) to evaluate surface smoothness. Their advanced

study showed that the acceleration data collected by smartphones is linearly related to IRI and changes in vehicle speed. Venkatesh *et al.*[13] proposed a system framework for pothole detection based on acceleration sensors. Zeng *et al.*[14] proposed the use of the built-in acceleration sensor of a smartphone to test road sections with serious surface damage at different driving speeds. Islam *et al.*[15] proposed the theory of using smartphones to test road conditions and converted the tested acceleration data of smartphone sensors into IRI through an algorithm. Wang and Guo[16] converted acceleration data tested by smartphones into indexes that can represent road conditions in a pilot project of the World Bank in Belarus. Stribling *et al.*[17] analyzed the effects of the vehicle type and speed on acceleration-fitted pavement characterization values by using the data of smartphones for different vehicles running at different speeds. However, there are major differences between highway and bicycle roads in their geometric alignment, driving speed, road performance requirements, and functional level.

In this study, a method of quantifying the roughness of bicycle paths using accelerometers, speedometers, and GPS is proposed and verified through experiments. It is possible to develop a method of increasing riding comfort by understanding the ride behavior of non-motor vehicles. It is of major practical significance to establish a system for bicycle road roughness evaluation to improve the environment for slow-moving traffic and promote people-oriented traffic by scientific methods.

2. Riding Profiler

2.1 Conceptual design

We set up a system for testing bicycle riding surface roughness. The test system comprises the bicycle as the carrier, which is combined with a KINGSIR speed sensor, a BWT901CL 3D high-precision acceleration sensor, and a BB10 GPS sensor, with a smartphone used as a data collector. A schematic diagram of the test system is shown in Fig. 1. The bicycle selected for the

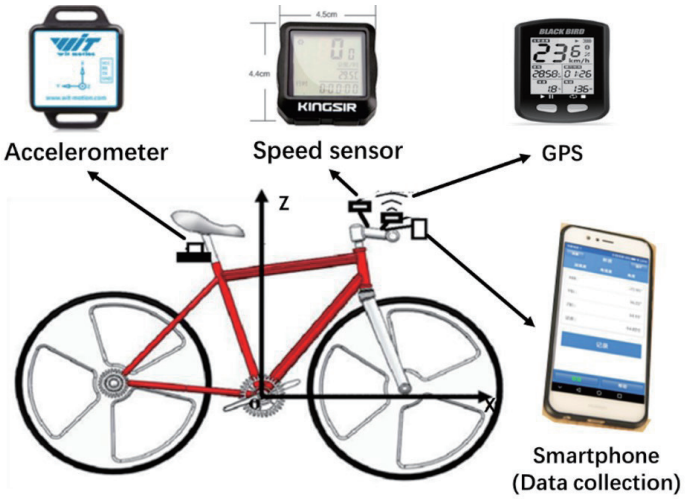

Fig. 1. (Color online) Schematic diagram of test system.

experiment is the "Halo Bicycle" commonly used for short- and medium-distance travel, with a wheel specification of 24 × 1.5 in and a tire pressure of 45 psi. The display of the KINGSIR cycle computer is installed on the front fork of the bicycle and its sensor is installed on the tire. The acceleration sensor is installed under the saddle. The speed display, GPS, and smartphone are installed on the handlebar for real-time observation during riding. In this system, the speed sensor (KINGSIR cycle computer) can measure the real-time riding speed in the range from 0.1 to 99.9 km/h with an accuracy of 0.1 km/h. The acceleration sensor can measure the vibration acceleration when riding, which can be used to calculate the smoothness of the traveled surface, then the ride comfort can be calculated with the 3D measuring range and an accuracy of 0.05. The GPS cycling computer can record the cycling route and give the position data of the test section with a measuring range of 0–9999 km and an accuracy of 0.01. All the sensors of this system can be wireless and are connected to a smartphone via Bluetooth, with the smartphone used to control data recording and storage and facilitate one-man operation when riding. In contrast to the roughness evaluation system for highways, there is no requirement to carry bulky instruments, a computer, or other equipment for this system, making it suitable for non-motor vehicle users.

2.2 Experimental design

To verify the test repeatability and multi-environmental application of the riding profiler, the test and verification of the system are completed in two stages. To eliminate the effects of the surrounding environment and the cyclist's perception of vibration and psychological factors on the test results, straight sections with dry pavement and high smoothness are selected in the test. The information of the phased test sections and the experimental variables are shown in Table 1. The three selected test sections are Guzong Road, Hucheng Ring Road, and Haigang Avenue. The pavement types are dense asphalt, porous concrete, and concrete block pavements. The road width is 3.5 m and the effective test length is 100 m.

To verify the repeatability of the test system, three experiments are conducted with the developed riding profiler ridden at 10 km/h on the same section of Hucheng Ring Road. In addition, to analyze the effects of the riding speed and pavement type on roughness evaluation, concrete block, porous concrete, and dense asphalt pavements with obvious texture differences are selected for tests at speeds of 10, 15, and 20 km/h. Because the bicycle is ridden by humans,

Table 1
Information and experimental variables of phased test sections.

	Location	Width (m)	Pavement type	Length (m)	Test speed (km/h)
Phase 1	Hucheng Ring Rd.	3.5	Porous concrete pavement	100	10
	Guzong Rd.	3.5	Dense asphalt pavement	100	10
Phase 2	Hucheng Ring Rd.	3.5	Porous concrete pavement	100	10/15/20
	Haigang Ave.	3.5	Concrete block pavement	100	10

there will inevitably be errors in the riding speed. However, in the experiment, the speed error is limited to within ±5%. Three tests are performed for each variable in all experiments.

2.3 Displacement based on vibration signal

Owing to the noise interference of various external and internal factors in the testing process, the acquired signal requires preliminary processing. The acceleration waveform should be corrected, and the noise and interference in the signal must also be eliminated before data analysis. The five-point moving average is used to denoise the original vertical acceleration data. The displacement component is obtained by integrating the Fourier component of the acceleration signal twice. The Fourier component of the acceleration signal at any frequency can be expressed as

$$a(t) = Ae^{jwt}, \tag{1}$$

where $a(t)$ is the Fourier component of the acceleration signal at frequency w, A is the coefficient corresponding to $a(t)$, and j is the imaginary unit.

When the initial velocity component is 0, the time integral of the acceleration signal component can be used to derive the velocity signal component,

$$v(t) = \int_0^t a(t)\,dt\,. \tag{2}$$

When the initial velocity and displacement components are both 0, the Fourier component of the acceleration signal is integrated twice to obtain the displacement component,

$$x(t) = \int_0^t \left[\int_0^t a(t)\,dt \right] dt, \tag{3}$$

where $x(t)$ is the Fourier component of the velocity signal at frequency w. Thus, the relationship between the two integrals in the frequency domain is

$$X = -\frac{A}{w^2}. \tag{4}$$

The numerical equation for the second integral can be expressed as

$$y(r) = \sum_{k=0}^{N-1} -\frac{1}{(2\pi k\Delta f)^2} H(k) X(k) e^{j2\pi kr/N}, \tag{5}$$

where

$$H(k)=\begin{cases}1, & f_d \le k\Delta f \le f_u \\ 0, & \text{other.}\end{cases} \tag{6}$$

Here, f_d and f_u are the lower and upper cutoff frequencies, respectively, $H(k)$ is a systematic function used for digital filtering, $X(k)$ is the Fourier transform of $X(r)$, and Δf is the frequency resolution.

After obtaining the displacement data, IRI can be obtained using Eq. (7), i.e., by dividing the cumulative vertical displacement by the measured distance L.

$$IRI = \frac{X}{L} \tag{7}$$

2.4 Repeatability test

To test the stability of the riding profiler, a pre-test of repeatability was carried out at a speed of 10 km/h along Hucheng Ring Road. The three sets of measured data are shown in Fig. 2; Fig. 2(a) gives the raw acceleration data and Fig. 2(b) exhibits the displacement after processing the original data. The three sets of experimental acceleration data are very well fitted with the displacement line chart, and the IRI values measured for the three sets are 1.31, 1.40, and 1.29 m/km with a standard deviation of 5.86×10^{-2} and a variance of 3.43×10^{-3}. According to the test results, the system can be used to obtain the measured data highly fitted with good repeatability and high stability.

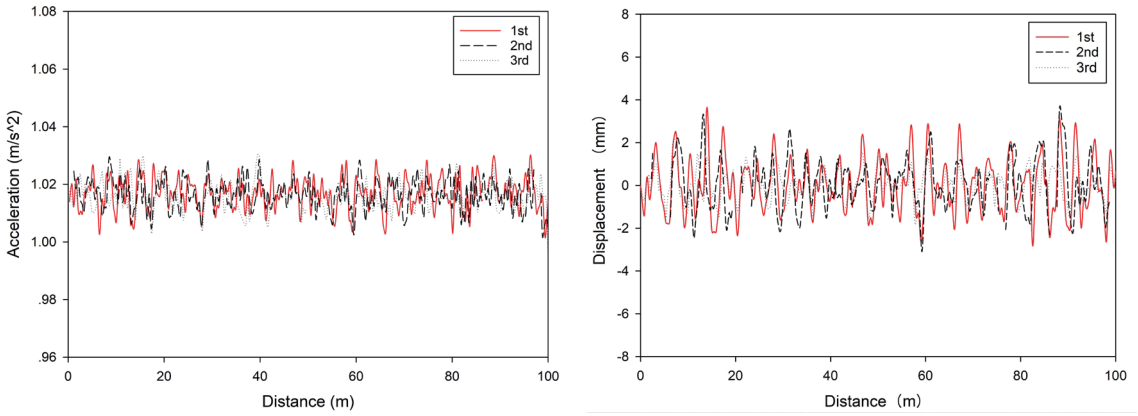

(a) (b)

Fig. 2. (Color online) Three sets of acceleration and displacement data for the same road section. (a) Acceleration data. (b) Displacement data.

3. Application of Riding Profiler

3.1 Effect of riding speed on roughness measurement

To analyze the effect of the riding speed on test results for roughness, the riding profiler is used for testing at speeds of 10, 15, and 20 km/h along Hucheng Ring Road. The test results are shown in Fig. 3. There is a small bump at about 80 m from the test starting point. The higher the riding speed, the greater the displacement variation will be, and the higher the riding speed, the stronger the vibration will be felt, greatly reducing the comfort. The range of displacement deviation during riding is kept within a small amplitude of ±5 mm, but the vibration is transmitted because the suspension system of the bicycle saddle is weak. Therefore, a change in displacement does not tend to be directly reflected in the ride comfort on a road surface. Table 2 shows the IRI values calculated at different riding speeds. The mean, variance, and standard deviation of IRI at different speeds differ slightly, which demonstrates that the test speed has little effect on the obtained IRI.

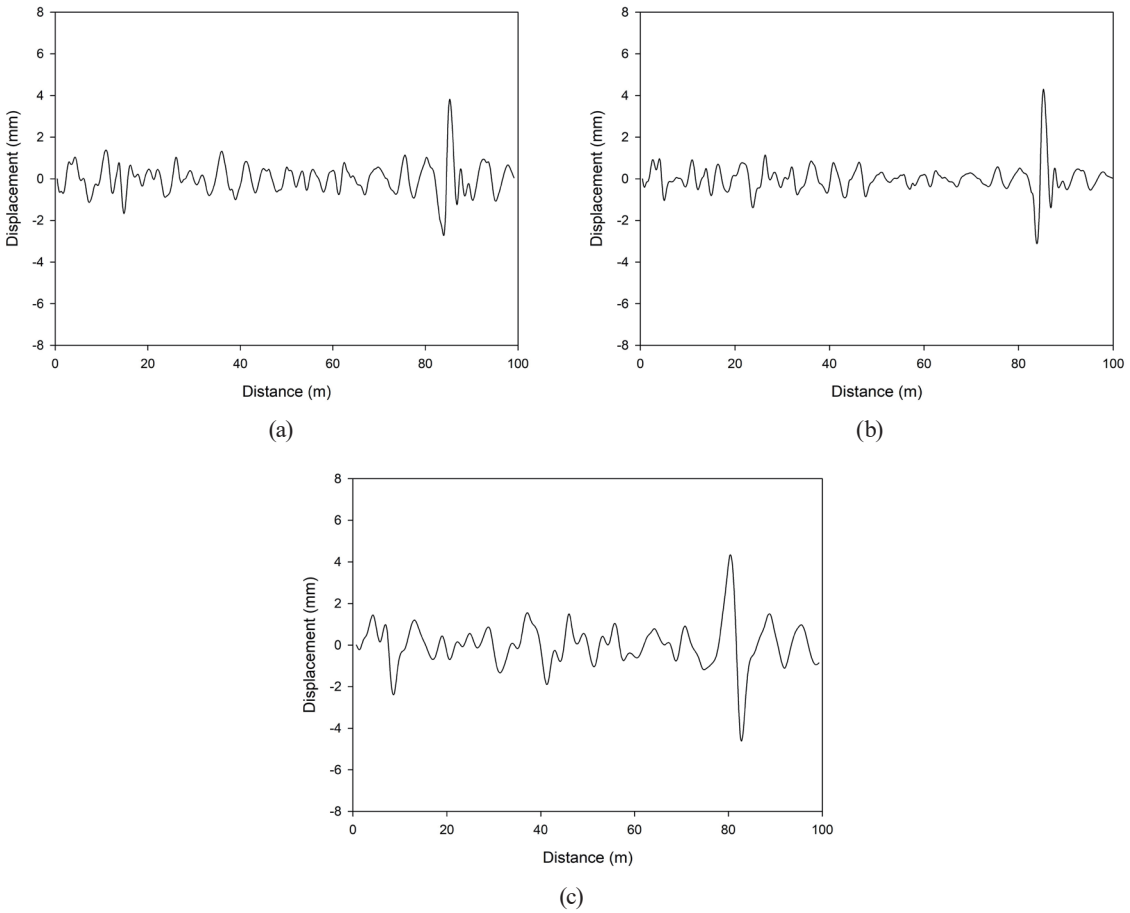

Fig. 3. Vertical displacement vs distance curves at different riding speeds. (a) Vertical displacement curve at 10 km/h. (b) Vertical displacement curve at 15 km/h. (c) Vertical displacement curve at 20 km/h.

Table 2
Comparison of IRI values at different speeds on the same road surface.

	Speed (km/h)	Mean	Variance	Standard deviation
IRI (m/km)	10	1.386	3.53×10^{-3}	5.71×10^{-2}
	15	1.392	3.27×10^{-3}	5.94×10^{-2}
	20	1.398	3.67×10^{-3}	6.05×10^{-2}

3.2 Effect of pavement type on roughness measurement

Riders have different riding responses to different types of pavement. To analyze the effect of the pavement type on surface roughness, the riding profiler is used for tests on dense asphalt, porous concrete, and concrete block pavements at a speed of 10 km/h. The vertical displacement variations are shown in Fig. 4.

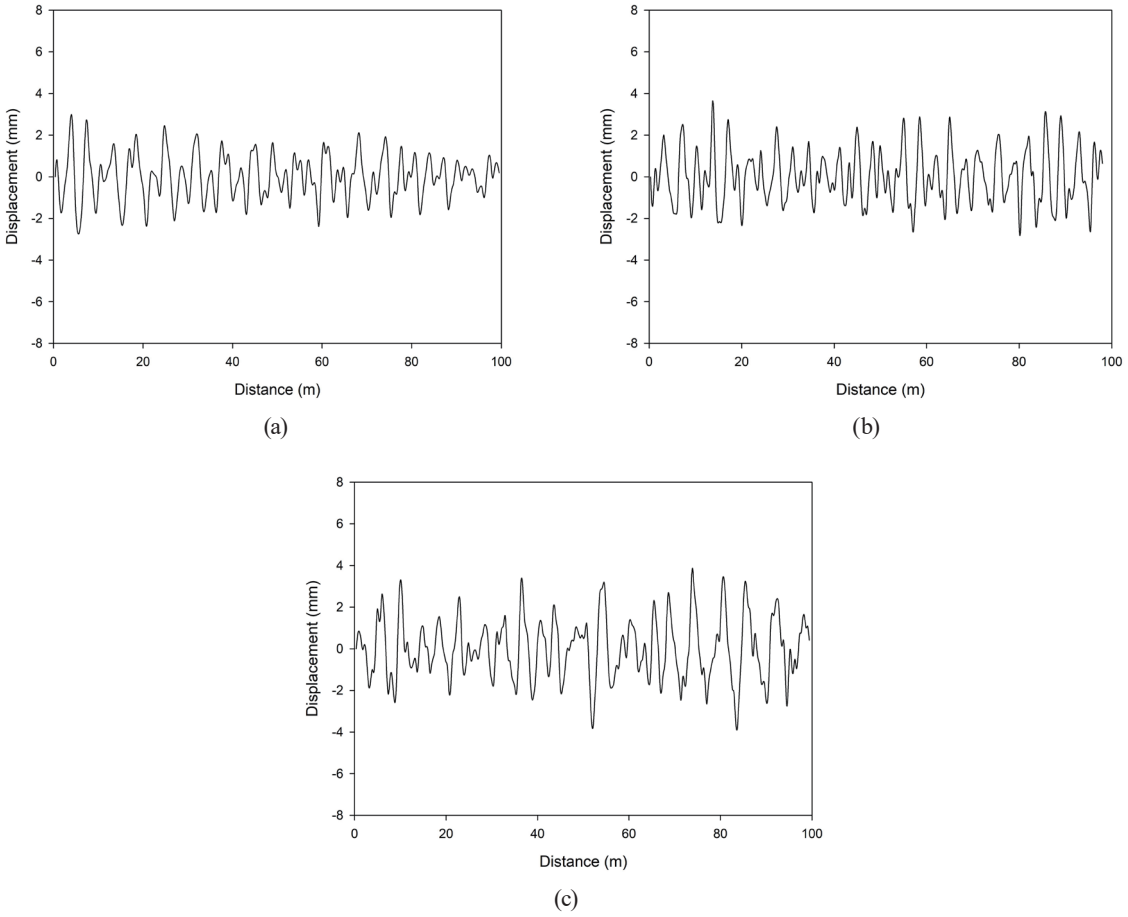

Fig. 4. Variation of vertical displacement on three different types of pavement at 10 km/h. (a) Variation of vertical displacement on dense asphalt pavement, (b) variation of vertical displacement on porous concrete pavement, and (c) variation of vertical displacement on concrete block pavement.

The displacement variation is largest for the concrete block pavement, followed by the porous concrete and dense asphalt pavements. Because of the low roughness of each surface, the displacement vibrations in the selected test sections are all within ±5 mm with a small variation range. However, during the riding test, different types of pavement will obviously induce different types of feedback in the form of vibration during riding. Because of its discontinuous surface structure, there are many joints between the blocks of concrete block pavement, leading to frequent acceleration changes and poor ride comfort. For porous concrete pavement, the existence of expansion joints increases its surface roughness, but it is much smoother than concrete block pavement. In contrast, dense asphalt pavement is poured integrally, giving it good consistency and a relatively good texture. The vertical displacement variation of a bicycle running on concrete block pavement is larger than that for porous concrete pavement, which in turn is larger than that for dense asphalt pavement. Therefore, the vertical displacement of riding varies with the type of pavement. Table 3 shows a comparison of IRI values on different types of pavement at the same speed. IRI is largest for concrete block pavement, followed by porous concrete pavement and then dense asphalt pavement. Therefore, the rougher the pavement, the greater its displacement and IRI.

4. Riding Comfort Evaluation

4.1 Acceleration interference

The impact of vibration on the human body depends on its frequency, intensity, direction, and duration, but each rider has a different tolerance to vibration, so there are large differences among riders. Because changes in acceleration have a direct impact on ride comfort, acceleration interference is often used as an index to evaluate comfort in the theory of vehicle ride comfort. Hölzel *et al.*[18] used acceleration interference to evaluate the impact of riding vibration on ride comfort when studying the comfort of riding bicycles on different types of pavement. Acceleration interference represents the frequency of acceleration and deceleration during riding. The greater the acceleration interference, the lower the ride comfort.[19,20] Acceleration interference is calculated as

$$a_w = \left[\frac{1}{T} \int_0^T a_w^2(t)\, dt \right]^{\frac{1}{2}}, \tag{8}$$

Table 3
Comparative analysis of IRI values on different types of pavement at the same speed.

	Type of pavement	Mean	Variance	Standard deviation
IRI (m/km)	Dense asphalt pavement	1.03	3.73×10^{-3}	6.11×10^{-2}
	Porous concrete pavement	1.33	3.42×10^{-3}	5.85×10^{-2}
	Concrete block pavement	2.27	6.7×10^{-3}	8.18×10^{-2}

where a_w is the vertical acceleration interference, $a_w(t)$ is the weighted acceleration time history, obtained by a filter network of the corresponding frequency weighting function $w(f)$, and T is the analysis time of vibration.

The frequency weighting function can be expressed as follows, with Hz as the unit of frequency.

$$w(f)=\begin{cases}0.5, & 0.5<f<2\\ f/4, & 2<f<4\\ 1, & 4<f<12.5\\ 12.5, & 12.5<f<80\end{cases} \tag{9}$$

4.2 Analysis on correlation of acceleration interference with roughness and speed

Pavement roughness is the main cause of vertical vibration, and the vibration of a riding bicycle changes with the speed. For this reason, multiple linear regression analysis is performed on the relationships among speed, roughness, and vertical acceleration interference. A 3D scatter plot of the three variables is illustrated in Fig. 5, where Eq. (10) is the regression equation of the variables. The three variables showed a strong correlation with a correlation coefficient R^2 of 0.97, and the significance test P value of the model equation is <0.05. Therefore, this linear regression can be considered as significant.

$$a_w = 0.121IRI + 0.003V - 0.161 \tag{10}$$

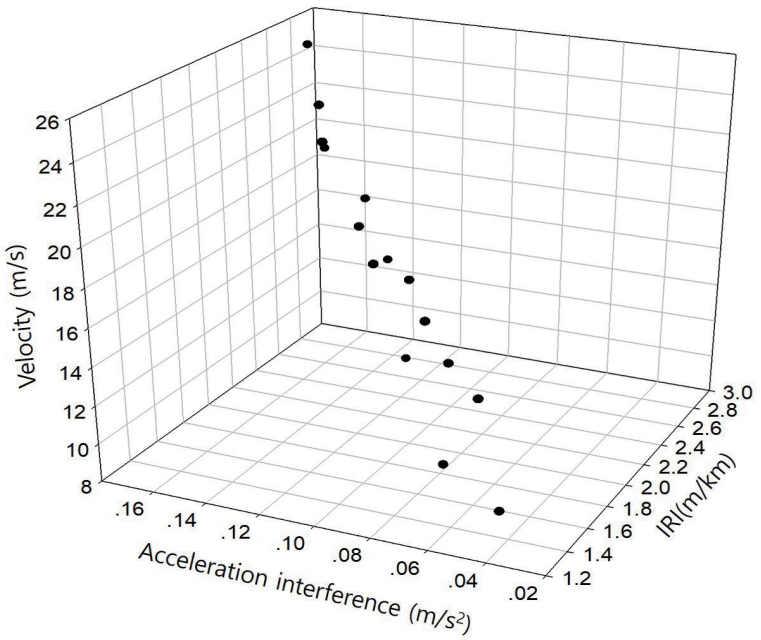

Fig. 5. 3D scatter plot of speed, roughness, and acceleration interference.

4.3 Riding comfort index for bicycle lanes

Seventeen sections of a rough bicycle lane are selected to analyze ride comfort using acceleration interference. Each road section is divided into three parts: smooth, transition, and rough parts. All the tests are performed at a speed of 10 km/h. The smooth part has low roughness and no distress, and the rider feels comfortable when riding on this part. The transition part connects the smooth and rough parts. When a rider passes through this part, they experience bumps, focusing their attention and causing discomfort. The rough part has high roughness with obvious distress. The rider feels uncomfortable and experiences bumps when riding on this part even for a short distance. The acceleration interference values of the 17 sections are shown in Table 4.

Hölzel *et al.*[18] pointed out that a human feels comfortable for an acceleration interference of less than 0.01 m/s^2, slightly uncomfortable for a value of 0.01–0.015 m/s^2, somewhat uncomfortable for a value of 0.015–0.02 m/s^2, uncomfortable for a value of 0.02–0.08 m/s^2, highly uncomfortable for a value of 0.08–0.35 m/s^2, and very highly uncomfortable for a value of more than 0.35 m/s^2. Next, we analyze the ride comfort on pavement in accordance with the comfort evaluation index for non-motor vehicles proposed by Hölzel *et al.*[18] The measured maximum acceleration interference values are 0.09 m/s^2 in the smooth part, 0.13 m/s^2 in the transition part, and 0.22 m/s^2 in the rough part, all of which fall under the standard of highly uncomfortable.

As can be seen from Table 4, the means of acceleration interference in the test sections are 0.07 m/s^2 for the smooth part, 0.11 m/s^2 for the transition part, and 0.20 m/s^2 for the rough part. On the basis of these values, a new comfort evaluation index for bicycle lanes is defined as shown in Table 5. A section with an acceleration interference of less than 0.07 m/s^2 is regarded

Table 4
Acceleration interference values (m/s^2).

Test section	Smooth part	Transition part	Rough part
Section 1	0.07	0.12	0.21
Section 2	0.05	0.10	0.20
Section 3	0.09	0.13	0.21
Section 4	0.07	0.10	0.19
Section 5	0.06	0.10	0.21
Section 6	0.08	0.12	0.19
Section 7	0.07	0.11	0.20
Section 8	0.07	0.10	0.20
Section 9	0.09	0.09	0.18
Section 10	0.06	0.12	0.21
Section 11	0.07	0.11	0.20
Section 12	0.09	0.12	0.20
Section 13	0.06	0.13	0.19
Section 14	0.06	0.10	0.18
Section 15	0.07	0.10	0.22
Section 16	0.09	0.11	0.21
Section 17	0.06	0.11	0.21
Mean	0.07	0.11	0.20

Table 5
Comfort evaluation index for bicycle lanes.

Acceleration interference a_w	Subjective perception
<0.07	Comfortable
0.07–0.11	Slightly uncomfortable
0.11–0.20	Uncomfortable
>0.20	Highly uncomfortable

Table 6
Acceleration interference and IRI of different pavement types.

	Dense asphalt pavement	Porous concrete pavement	Concrete block pavement
a_w (m/s^2)	0.07	0.09	0.21
IRI (m/km)	1.22	1.37	2.23

as comfortable, one with a value between 0.07 and 0.11 m/s^2 is regarded as slightly uncomfortable, one with a value between 0.11 and 0.20 m/s^2 is regarded as uncomfortable, and one with a value above 0.20 m/s^2 is regarded as very uncomfortable.

To evaluate the riding comfort of different pavement types, this index is utilized to test and verify concrete block, dense asphalt, and cement pavement sections of roads in good condition. The calculated acceleration interference values are given in Table 6. The acceleration interference increases with IRI and is largest for the concrete block pavement. Compared with porous concrete pavement, the surface of dense asphalt pavement is smoother and the measured acceleration interference and IRI values are smaller. According to the comfort index for bicycle lanes established in this paper, dense asphalt pavement falls under the standard of comfortable, porous concrete pavement under that of slightly uncomfortable, and concrete block pavement under that of very uncomfortable, which may be mainly caused by the many joints between the blocks.

5. Conclusion

As the number of bicycle users increases, the demand for high-quality bicycle lanes is increasing. In this study, a riding profiler was designed and developed to evaluate the roughness of a bicycle riding surface. As a result of experiments with speed as a variable, the effect of speed on vertical displacement was found to be limited. However, it affects the degree of turbulence, with a higher speed resulting in more turbulence.

To analyze the effect of the pavement type on roughness, dense asphalt, porous concrete, and concrete block pavements were evaluated. The results show that the vertical displacement variation is largest when riding on concrete block pavement, followed by porous concrete and dense asphalt pavements. However, the variation range of the vertical displacement is small and remains within ±5 mm, which is related to the acceleration variation frequency. Because of this characteristic, we proposed the use of acceleration interference as an evaluation index for ride comfort on the basis of the results of repeated measurements of multiple sections. According to the measured data and the rider's perception feedback, riding comfort index ranges based on

acceleration interference are given, with comfortable defined as an acceleration interference of less than 0.07 m/s^2, slightly uncomfortable as a value of 0.07–0.11 m/s^2, uncomfortable as a value of 0.11–0.20 m/s^2, and very uncomfortable as a value of more than 0.20 m/s^2.

On the basis of these limited test results, the applicability of an efficient riding profiler was verified. Furthermore, the correlation between acceleration interference and IRI was shown. In the future, research on algorithm development is needed so that the results of various additional experiments and acceleration interference values can be represented as IRI.

Acknowledgments

This research was supported by the National Natural Science Foundation of China (No. 51808334) and the Business Creation Support Program through the Ministry of Land, Infrastructure and Transport of the Korean Government under Grant 22TBIP-C160754-02.

References

1 American Society for Testing and Material: Standard Terminology Relating to Vehicle-Pavement Systems, ASTM E867 (West Conshohocken, PA, 2012).
2 W. Liu, T. F. Fwa, and Z. J. Zhao: Transp. Eng. **131** (2005) 120. https://doi.org/10.1061/(ASCE)0733-947X(2005)131:2(120)
3 M. W. Sayers and S. M. Karamihas: The Little Book of Profiling: Basic Information about Measuring and Interpreting Road Profiles (University of Michigan Transportation Research Institute, Ann Arbor, 1998).
4 B. Zhou, X. Zhu, and W. Sun: J. Hefei Univ. Technol. (Natural Science) **9** (2004) 1095. https://www.semanticscholar.org/paper/Application-of-vehicular-bump-integrator-inthe-Wen/ae4d2c5fb6a2d325ce4832019760cb501d89fa81
5 B. Suksawat: Proc. 2011 Int. J. Control Autom. Syst., 11th Int. Conf. IEEE. (2011) 799.
6 G. Cantisani and G. Loprencipe: J. Transp. Eng. **136** (2010) 818. https://doi.org/10.1061/(ASCE)TE.1943-5436.0000143
7 E. P. Dennis, Q. Hong, R. Wallace, W. Tansil, and M. Smith: Transp. Res. Rec. **2460** (2014) 31. https://doi.org/10.3141/2460-04
8 V. Douangphachanh and H. Oneyama: J. East. Asia Soc. Transport. Stud. **10** (2013) 1551. https://doi.org/10.1186/1687-1499-2014-114
9 A. Mednis, G. Strazdins, R. Zviedris, G. Kannoirs, and L. Selova: Proc. 2011 Int. Conf. Distributed Computing in Sensor Systems and Workshops (IEEE, 2011). https://doi.org/10.1109/DCOSS.2011.5982206
10 N. Divya and D. Bansal: Int. J. Electron. Electr. Eng. **7** (2014) 679. https://www.ripublication.com/irph/ijeee_spl/ijeeev7n7_07.pdf
11 A. González, E. J. O'brien, Y. T. Li, and K. Cashell: Veh. Syst. Dyn. **46** (2008) 485. https://doi.org/10.1080/00423110701485050
12 V. Douangphachanh and H. Oneyama: EURASIP J. Wireless Commun. Network **114** (2014). https://doi.org/10.1186/1687-1499-2014-114
13 S. Venkatesh, E. Abhiram, S. Rajarajeswari, K. M. S. Kumar, S. Balakuntala, and N. Jagadish: Proc. 2014 7th Int. Conf. Mobile Computing and Ubiquitous Networking (ICMU, Singapore) (2014). https://doi.org/10.1109/ICMU.2014.6799066
14 H. Zeng, H. Park, M. D. Fontaine, B. L. Smith, and K. K. McGhee: Transp. Res. Rec. **2523** (2015) 133. https://doi.org/10.3141/2523-15
15 S. Islam, W. G. Buttlar, R. G. Aldunate, and W. Vavrik: Transp. Res. Rec. **2457** (2014) 30. https://doi.org/10.3141/2457-04
16 W. Wang and F. Guo: Proc. 2016 95th Annu. Meeting of the Transportation Research Board (Washington, D.C., TRB 2016) 16-2116.
17 J. W. Stribling, W. G. Buttlar, S. Islam, and W. R. Vavrik: Proc. 2017 96th Annu. Meeting of the Transportation Research Board (Washington, D.C., TRB2017) 17-05717.
18 C. Hölzel, F. Höchtl, and V. Senner: Procedia Eng. **34** (2012) 479. https://doi.org/10.1016/j.proeng.2012.04.082

19 J. S. Eiscle, Y. Y. Haimes, N. J. Carber, D. Li, J. H. Lambert, P. Kuzminski, and M. Chowdhury: Reliab. Eng. Syst. Saf. **54** (1996) 65. https://doi.org/10.1016/S0951-8320(96)00085-3
20 S. M. Easa: J. Transp. Eng. **129** (2003) 127. https://doi.org/10.1061/(ASCE)0733-947X(2003)129:2(127)

About the Authors

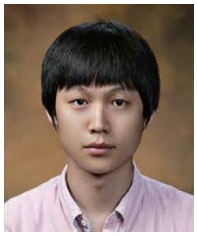

Wuguang Lin received his B.S. degree from Changchun Institute of Technology, China, in 2007 and his Ph.D. degree from Chung-Ang University, Korea, in 2015. From 2015 to 2018, he was an assistant professor at Shanghai Maritime University, China. Since 2019, he has been an associate professor at Shanghai Maritime University. His research interests are in pavement structure design and pavement condition monitoring. (wglin@shmtu.edu.cn)

Yu Dong received his B.S. degree from Shanghai Maritime University, China, in 2019. Since 2020, he has been a research assistant at Shanghai Maritime University. His research interests are in the design of transportation systems and pavement condition monitoring. (201930610046@stu.shmtu.edu.cn)

Xue Ren received her B.S. degree from Shandong Jiaotong University, China, in 2018 and her M.S. degree from Shanghai Maritime University, China, in 2020. Since 2020, she has been an assistant teacher at Zhibo Education. Her research interests are in the planning and design of transportation systems. (17862956864@163.com)

Hao Han received his B.S. degree from Inner Mongolia University of Technology, China, in 1989 and his M.S. and Ph.D. degrees from Tongji University, China, in 1997 and 2002, respectively. From 2002 to 2004, he was a research fellow at Tongji University. Since 2005, he has been a professor at Shanghai Maritime University. His research interests are in the planning and design of transportation systems. (haohan@shmtu.edu.cn)

YooSeok Jung received his B.S. and M.S. degrees from Chung-Ang University, Korea, in 2012 and 2014, respectively. Since 2015, he has been a senior researcher at Korea Institute of Civil Engineering and Building Technology. His research interests are in IoT, monitoring, and sensors. (yooseok@kict.re.kr)